A methodology for estimation of the specific rock energy index using corrected down-the-hole drill monitoring data

Luis E. Izquierdo and Luciano E. Chiang

A methodology developed to estimate with accuracy the instantaneous specific rock energy using corrected down-the-hole (DTH) drill monitoring data is presented. A specific rock energy profile can be generated for every hole, and thus a drilling site can be mapped for this index. A special data acquisition system was developed to measure and register the following operational variables: penetration rate, torque, hole depth, pull-down force, air pressure, revolutions per minute (rpm) and the hammer percussion frequency, the latter obtained by sound recording and signal processing. The measured data are fed into two simulation models that estimate the power absorbed by the rock through impact, and then the specific rock energy index. The first of these models simulates the thermodynamic cycle of the DTH hammer, rendering the piston kinetic energy at impact, impact velocity as well as impact frequency. The second model is used for stress wave propagation analysis to estimate the effective energy delivered to the rock. Correlations were found between the specific rock energy and penetration rate, and between the specific rock energy and impact frequency, as well as between the penetration rate and applied torque, and between the penetration rate and impact frequency.

Luis E. Izquierdo (leiv@ing.puc.cl) and Luciano E. Chiang (lchiang@ing.puc.cl) are at the Departamento de Ingeniería Mecánica, Pontificia Universidad Catolica de Chile, 4860 Vicuna Mackenna Ave, Casilla 306 Correo 22, Santiago, Chile.

 Manuscript received 1 October 2002; accepted in final form 28 May 2004.

Keywords: Down-the-hole hammer, drilling monitoring, hammer percussion frequency, specific rock energy, percussion drilling, air drilling

INTRODUCTION

The operation of rock drilling systems is an important issue in many industries such as mining, construction, petroleum and water well drilling. Due to its economic importance, it has motivated many research studies; recently, monitoring systems have been used to understand rock drilling better. In such systems, the variables most commonly measured are: penetration rate, penetration depth, torque, rotation speed (RPM), pull-down (feed force) and the air pressure. The analysis of these data has provided important information about the drilled rock mass such as hardness, fracturing and weathering.[15] It has permitted the location of rock boundaries, rock-type boundaries to name the most important, and it has helped in blast hole array design.[15,18,20]

One advantage of drill monitoring is the possibility to extract valuable information without causing disturbances in the drilling process. Monitoring is considered an important necessary step prior to the automation of the entire drilling process[2] because it helps to understand better how the different parameters affect rock drilling. Rock-drill monitoring can be used to detect anomalies in the hammer operation thereby helping to avoid potentially disastrous situations such as stalling.

THE DATA ACQUISITION SYSTEM

For the purpose of this research, the authors developed in-house, a computer-based monitoring system. This decision was taken for both economic and technical reasons: (i) available special-purpose commercial systems are high-priced; and (ii) generally for technical and legal reasons, the vendors do not allow modifications such as those this research required. The data acquisition and processing system development took more than a year of design and testing. The resulting system consists of several different sensors connected to an industrial computer that processes and stores the incoming data. To measure torque, pull-down and air pressure, pressure transducers were connected to the corresponding fluid lines on the drill rig as shown in Figure 1. Penetration

Nomenclature: A, hole area (m^2); E_{Impact}, impact energy (piston contribution) (J); E_{Torque}, torque energy (J); E_{Thrust}, thrust energy (J); e, piston impact restitution coefficient; F, percussion frequency; $F_{Pull\text{-}down}$, applied pull-down force (weight on bit) (N); F_{Thrust}, thrust force (N); m_{Piston}, piston mass (kg); SRE, specific rock energy ($J\,cm^{-3}$); Pow_{Hammer}, hammer power (W); V_{Impact}, piston impact velocity ($m\,s^{-1}$); $V_{Penetration}$, penetration rate ($m\,s^{-1}$); $Torque$, torque applied to the hammer (N m); $W_{Rods\text{-}hammer}$, rods and hammer weight (N); ω, hammer angular velocity ($rad\,s^{-1}$); Δt, time increment; $\Delta\theta$, hammer spin angle increment; Δx, hammer displacement increment; ΔVo, rock volume increment

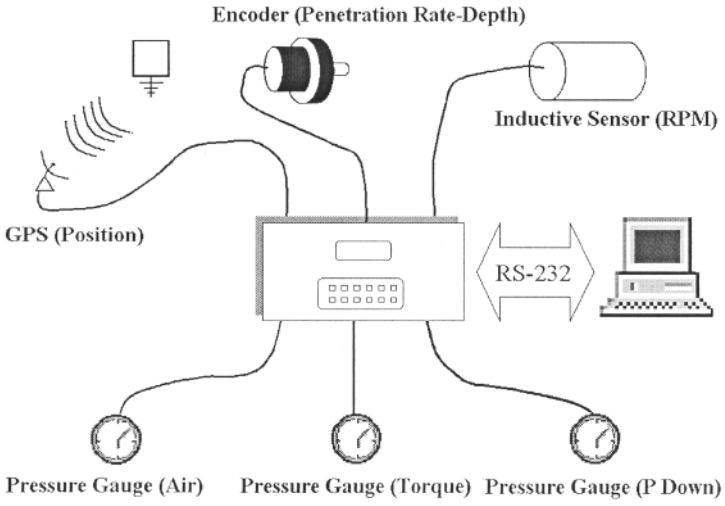

1 Schematic of the data acquisition system

rate and depth were measured using an optical encoder connected to the feed (displacement) chain of the drilling rig. A proximity sensor was used to measure rotation speed. The position of each hole in space was recorded using a GPS receiver. Finally, the hammer impact frequency was extracted from the post-test analysis of sound recordings made during *in situ* hammer operation sound recordings.

The results reported in this work were obtained during drill tests carried out at a diorite quarry located in the commune of Quilicura (Chile). Vertical holes were drilled with an Ingersoll Rand DM-45 drilling rig on which the developed monitoring system was mounted. Five- and six-inch diameter Puma DTH hammers supplied by Drillco Tools were used. These were equipped with 5·5- and 6·5-inch diameter drill bits, respectively. The system was set to store data every 5 cm of hole length. A total of 400 m of drilled holes considered representative of the rock mass were selected for the present discussion.

FORMULATION OF THE SPECIFIC ROCK ENERGY INDEX USING DTH DRILLING DATA

The specific rock index (SRI) quantifies the energy necessary to remove a given volume of rock. In the early 1960s, it was proposed by Teale[21] as a way to determine the amount of energy required to drill a specific volume of rock, using roller cone-bits. Roller cone sits are generally used to drill in low-to-medium hardness rock formations. Hustrulid,[7,8] on the other hand, used an SRE index obtained by laboratory tests to estimate the penetration rate in percussive drilling.

Other authors have extensively explored the use of the specific energy as an index to characterise the ease of rock removal as well. More recently, Thuro[22,23] applied a similar index (the destruction work index) to drifter hammers used in underground horizontal rock drilling. He found a strong correlation of this index, defined as the area under the stress–strain curve of the rock obtained from unconfined compression tests, and the penetration rate.

In this study, the SRE index is developed using DTH drilling data. This is not simple because it is necessary to account for the energy supplied by three separate sources – impact, rotation and pull-down – in order to determine the energy effectively absorbed by the rock. Thus, an in-depth knowledge of the DTH hammer drilling operation is required.

If the SRE index can be computed from drill monitoring data, then it can be used as a local drillability index to map and characterise the rock mass at the given drilling site.[15,18] Measured variations in the value of the index can be helpful in identifying the boundaries between different rock formations. It also can be indicative of a rock mass with a high degree of geological alteration, something that often occurs in mineral deposits.[18]

The SRE index is defined as the amount of energy (J) needed to remove a unit volume of rock. To derive an expression for the SRE, it is considered that the energy required to fragment the rock (E_{Rock}) is entirely provided by the drilling system. Hence:

$$E_{Rock} = E_{DTH\ system}$$

The energy absorbed by the rock in a short time interval can be written as:

$$\Delta E_{Rock} = SRE \bullet \Delta V_o \qquad \text{Eq. (1)}$$

where $\Delta V_o = A \times \Delta x$ is the volume of rock removed when generating a hole of cross-sectional area A and depth Δx.

Recalling that the energy provided by the drilling system comes from three separate sources – impact, torque and thrust – then:

$$E_{DTH\ System} = E_{Impact} + E_{Torque} + E_{Thrust} \qquad \text{Eq. (2)}$$

Therefore, it is possible to write the following expression for the SRE:

$$SRE = \frac{\Delta E_{Rock}}{A \bullet \Delta x} = \frac{\Delta E_{Impact}}{A \bullet \Delta x} + \frac{\Delta E_{Torque}}{A \bullet \Delta x} + \frac{\Delta E_{Thrust}}{A \bullet \Delta x} \qquad \text{Eq. (3)}$$

The ΔE_{Impact} increment can be approximated as the product of the average impact power supplied by the hammer (Pow_{Hammer}) and the duration of the time interval (Δt) over which the volume of rock (ΔV_o) is removed. The energy increment provided by the rotation torque (ΔE_{Torque}) can be approximated as the product of the average applied torque and the spin angle increment ($\Delta\theta$) during the same time interval. Finally, the product of the average thrust force (F_{Thrust}) and the displacement interval (Δx) accounts for the energy supplied by the thrust force (ΔE_{Thrust}). It is important to note that the thrust force considers both the pull-down force supplied by the drilling rig, and the weights of the rods and the hammer. It is assumed that the depth interval is selected conveniently so that the measurements are representative of such an interval. Then it is possible to write:

$$\Delta E_{Hammer} = Pow_{Hammer} \bullet \Delta t$$

$$\Delta E_{Torque} = Torque \bullet \Delta\theta \qquad \text{Eq. (4)}$$

$$\Delta E_{Thrust} = F_{Thrust} \bullet \Delta x$$

$$F_{Thrust} = F_{Pull-down} + W_{Rods-Hammer}$$

Substituting each term in Equation (4) into Equation (3) gives:

$$SRE = \frac{Pow_{Hammer} \bullet \Delta t}{A \bullet \Delta x} + \frac{Torque \bullet \Delta\theta \bullet \Delta t}{A \bullet \Delta x \bullet \Delta t} + \frac{F_{Thrust}}{A} \qquad \text{Eq. (5)}$$

Introducing the penetration velocity ($V_{Penetration}$) and the angular velocity (ω):

$$V_{Penetration} = \frac{\Delta x}{\Delta t} \qquad \varpi = \frac{\Delta\theta}{\Delta t} \qquad \text{Eq. (6)}$$

Then, an expression to compute directly the SRE index (in J m^{-3}) is:

$$SRE = \frac{Pow_{Hammer}}{A \bullet V_{Penetration}} + \frac{Torque \bullet \omega}{A \bullet V_{Penetration}} + \frac{F_{Thrust}}{A} \qquad \text{Eq. (7)}$$

In Equation (7) the *Torque*, F_{Thrust}, ω and $V_{Penetration}$ magnitudes can be estimated from sensor readings. Therefore, in order to compute the SRE index using Equation (7), only the effective power Pow_{Hammer} transferred to the rock by impact remains to be identified. This term turns out to be the most significant of all, so that an accurate computation of Pow_{Hammer} is of paramount importance in obtaining a trustworthy value of the SRE index. For this purpose, the magnitude of Pow_{Hammer} will be computed from the following expression:

$$Pow_{Hammer} = Pow_{Raw} \bullet \eta_{Transmission} \qquad \text{Eq. (8)}$$

where Pow_{Raw} is the raw power developed by the pneumatic hammer engine, which is the piston impact energy times the impact frequency. The magnitude of Pow_{Raw} depends on the thermodynamic behaviour of the hammer, that is to say how efficiently the high-pressure air energy is converted into kinetic energy of the piston at impact. The impact between the piston and drill bit generates a stress wave that propagates toward the bit–rock hammer interface. Depending on the geometry of the hammer components and the mechanical properties of the rock, a percentage of the stress wave energy is actually absorbed by the rock, causing its failure, and the remaining is reflected and dissipated by the hammer itself and the supporting structure. The magnitude of $\eta_{transmission}$ takes into account these stress-wave propagation effects.

Chiang *et al.*[3–5] have developed computational models to compute the magnitude of the terms Pow_{Raw} and $\eta_{transmission}$ in Equation (8). A thermodynamic model of the hammer permits the computation of Pow_{Raw}. A second model allows one to compute the stress-wave transmission efficiency $\eta_{transmission}$. For the purpose of clarity, these models will be briefly described. A discussion of both models can be found in Appendices A and B.

THERMODYNAMIC MODEL OF A DTH HAMMER

In order to determine the contribution of impact power in the drilling performance of a DTH hammer, a thermodynamic model is required to calculate impact energy per blow, and impact frequency. The impact power developed by a DTH hammer originates from air supplied at high pressure. The balance of pressures in the front and rear chambers in a DTH hammer causes alternate up and down motion of a piston (see Fig. 2). At the end of the forward stroke, the moving piston impacts a drill bit, initiating a stress wave that travels towards the rock.

To simulate the thermodynamic operation of the DTH hammer, a model developed by Chiang and Stamm[5] was used. This relates air pressure, piston impact velocity, piston rebound velocity and impact frequency for a given DTH hammer geometry. It is important to note that the rock behaviour in this model is taken into account by an impact restitution coefficient *e* between the piston and drill bit.

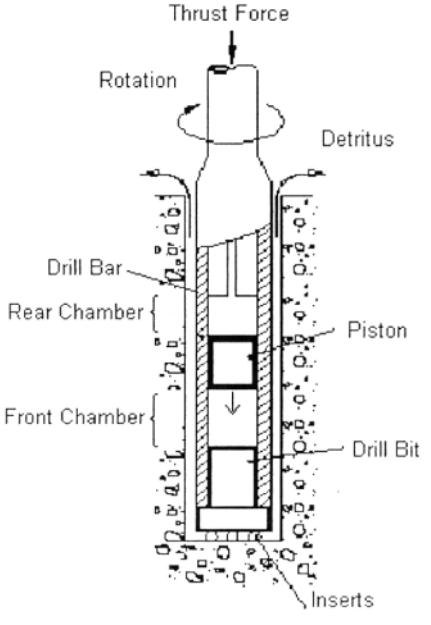

2 DTH hammer schematics

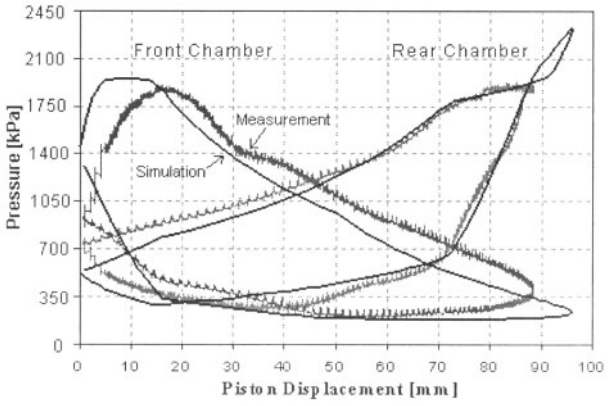

3 Actual and predicted front and rear chamber pressure versus piston displacement diagrams

$$e = \frac{piston\,'rebound'\,velocity}{piston\,impact\;factor}$$

The term e can be determined by simulation using a stress-wave propagation model developed by Chiang *et al.*,[3,4] described in the following section, or by experimental measurements. Hence, the thermodynamic model and the stress wave propagation model are coupled by parameter e.

This thermodynamic model has been experimentally validated for a number of DTH hammers in an experimental test bench. For example, Figure 3 shows the simulated pressure versus displacement diagram for the front and rear chambers of a DTH hammer. The actual pressure versus displacement diagrams obtained experimentally are included for comparison.

The model as well as laboratory and field measurements reveal that the predominant variable in the operation of any DTH hammer is the input air pressure. Figure 4 shows the raw power generated versus restitution coefficients for different air input pressure for a given hammer. Note that the predicted raw hammer power does not vary substantially with the restitution coefficient of the rock (Fig. 4), allowing one to conclude that rock behaviour has little effect on the raw power developed by the hammer.

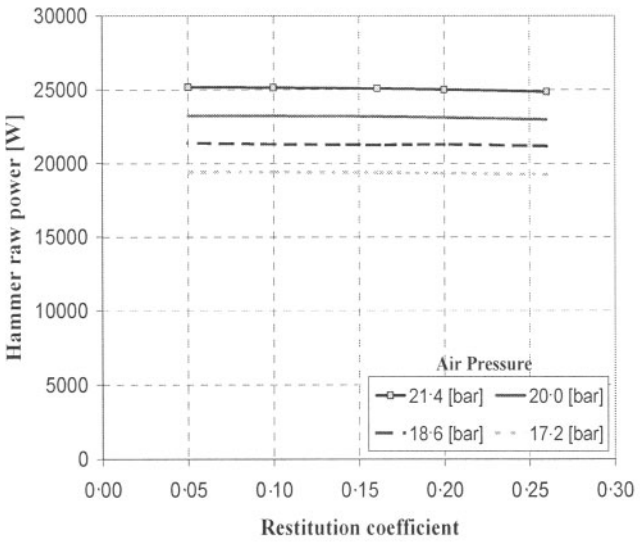

4 Hammer raw power versus restitution coefficient

The corresponding impact and rebound velocities and impact frequencies (percussion frequency) are shown in Figures 5–7, respectively. With these results and considering the fact that the raw power (maximum available power) of a DTH hammer is obtained as the product between the piston kinetic energy difference (impact and the rebound, the last represented by e^2) and the percussion frequency, it is possible to compute the raw power:

$$Pow_{Raw} = \frac{1}{2} \bullet m_{Piston} \bullet V_{Impact}^2 \left(1 - e^2\right) \bullet F \qquad \text{Eq. (9)}$$

An increase of the air pressure produces an increase of the impact velocity, which is independent of the restitution coefficient, as shown in Figure 5. A linear dependence was observed with the piston rebound velocity (Fig. 6).

Despite the fact that the rock behaviour simultaneously affects both the impact energy and the impact frequency, this occurs in such a way that the raw impact power delivered by the hammer (as shown in Figs. 5–7) remains basically constant for a given input air pressure. In fact, according to computer simulations

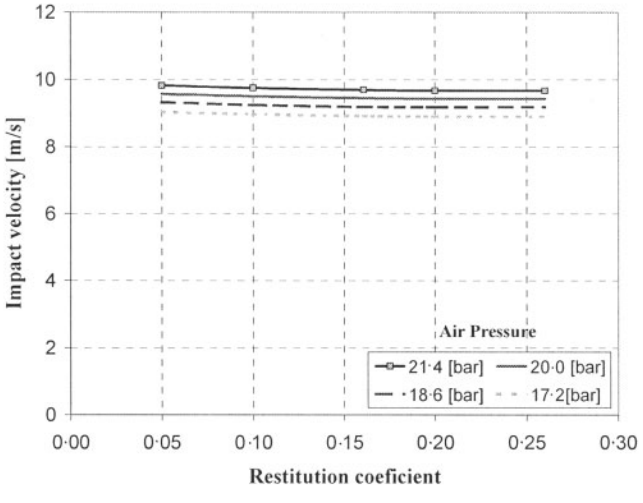

5 Piston impact velocity versus restitution coefficient

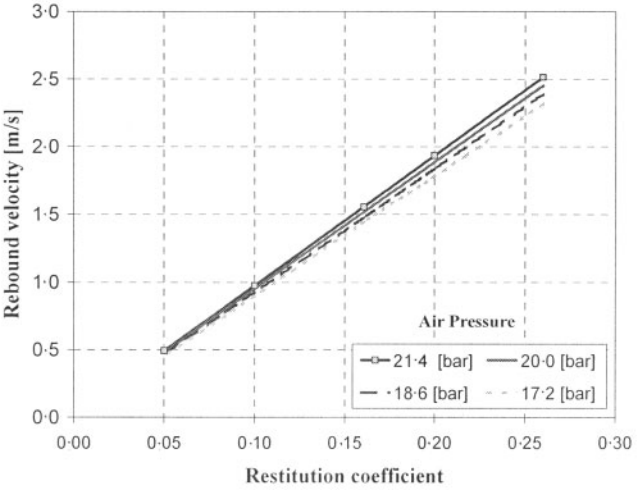

6 Variation of the piston rebound velocity versus restitution coefficient

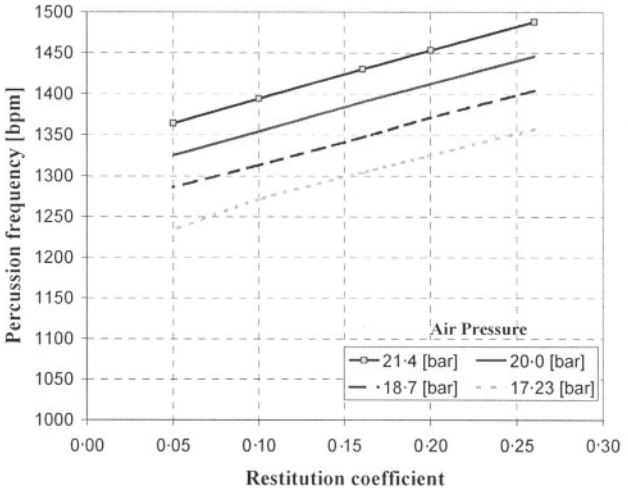

7 Percussion frequency in blows per minute (bpm) versus restitution coefficient

and also to field measurements, the impact frequency will increase (Fig. 7) as the rock becomes harder, that is to say when the penetration rate decreases. This frequency increment is compensated by a decrease in the piston kinetic energy transferred by impact (by way of an increase in the magnitude of the restitution coefficient e). This means that the overall raw power developed by the hammer does not change significantly for a wide range of values of the restitution coefficient, and hence for a wide range of medium-to-hard rock types being drilled.

This can be explained in terms of the piston cycle. If the restitution coefficient is low, then the reflected velocity is smaller. If the initial return velocity is less, the return piston cycle will increase with time. Thus, a low value of the restitution coefficient causes a decrease in the impact frequency and *vice versa*.

STRESS-WAVE PROPAGATION MODEL

The drill bit interacts with the rock mass through tungsten carbide inserts (Fig. 2). When the stress wave reaches the bit–rock interface, energy is transferred to the rock causing its fragmentation. Then, the cuttings are removed by the airflow exiting the hammer.

The raw power developed by the hammer is not transferred completely to the rock because in transferring energy, by means of a stress wave, there is a loss due to reflection and also due to friction at drill bar joints.

An algorithmic model developed by Chiang and Elías[4] permits the estimation of the efficiency of stress-wave transmission between the piston and drill bit and between the bit and rock mass. This model is based on the linear impulse–momentum principle. The geometry and material of the piston and of the bit must be specified, as well as a reference force–penetration curve for the bit–rock combination used. The latter is obtained experimentally. The stress-wave transmission model has been experimentally validated for a number of piston–bit–rock configurations by measuring stresses at selected sections in a pneumatic gun specially designed to investigate the effect. A similar method to estimate the efficiency of stress-wave transmission has been proposed by Lundberg[10–12] and by Pang[14]. Rossmanith *et al.*[17] have proposed a finite difference method to solve this problem.

In Figure 8, the results of experimental stress measurements in a pneumatic canon are shown. In this case, a piston at a velocity of 10 m s^{-1} impacts a stationary bit which, at the other end, is in contact with a rock specimen. Strain gauges are placed at different sections of the bit to record the stress-wave pattern. Both the model and theoretical stress-wave patterns are included in Figure 8 for comparison.

The efficiency of the energy transmission for a given piston–bit configuration can be estimated using the described model. Hence, a representative value of $\eta_{transmission}$ can be obtained by computer modelling.

Through the use of the thermodynamic and the impact models previously described, it is possible to estimate with adequate accuracy the energy and power (Pow_{Hammer}) actually transmitted to the rock by impact for a given working pressure. By substituting this

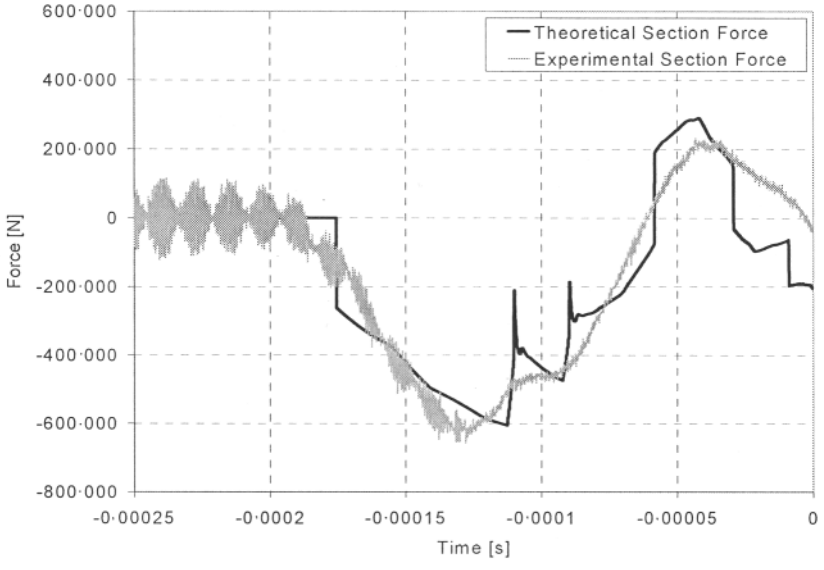

8 Experimental versus theoretical comparison of stress

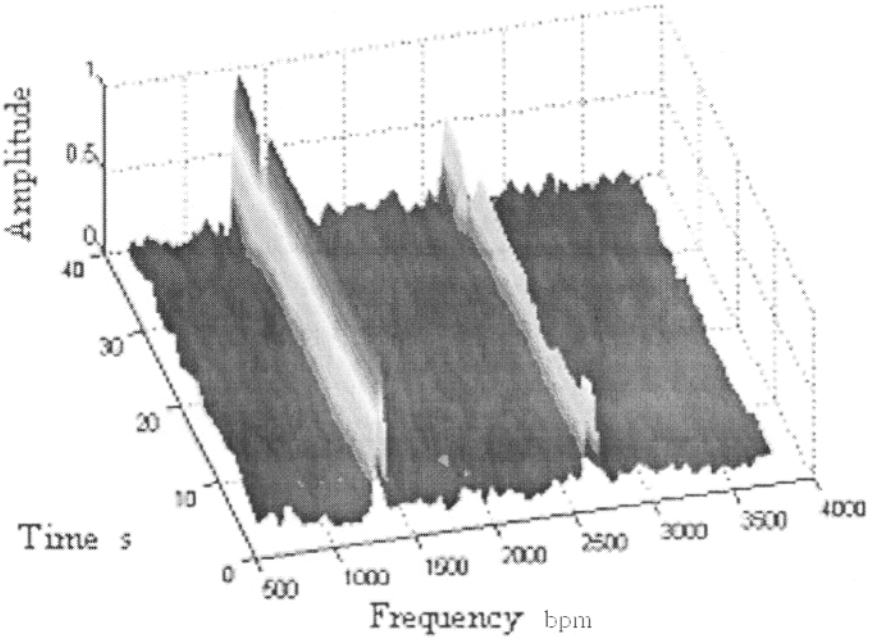

9 Spectogram representing the frequency, amplitude and time variation of a signal along a part of a drilled hole

known value in Equation (7), the corresponding complete SRE index can be obtained.

IMPACT FREQUENCY MEASUREMENT

The hammer percussion frequency has also been measured and analysed in order to check the estimated values of the frequency given by simulation, and to study its behaviour (i.e. variability) during rock drilling. The impact frequency is obtained from the analysis of sound recordings of the hammer in operation.

Measurements of frequency show that the range of variability is small[5] (about 160 blows per minute or 10%; Fig. 13). However, through the continuous monitoring of the impact frequency one can examine whether the variability can be correlated to other operational variables, such as torque, rotation speed, thrust force and penetration rate.

The strategy followed in the frequency analysis is to process short periods of the signal, in this case windows of 1·5–2 s. For each window, an average frequency is calculated. Time–frequency analysis[1,6] is used because it gives better results than alternatives such as signal peak detection that are affected strongly by signal noise. In particular, we used the Short Time Fourier Transform (STFT),[16] that involves calculating the Fourier transform of short signal portions using a window that slides over time along the signal. The results are visualised in the form of a spectrogram, a 3-D representation of the frequency, amplitude and time variation of a signal. In Figure 9, a spectrogram along a part of a drilled hole is shown.

DISCUSSION

SRE profile and individual source contributions

The specific rock energy profile, computed using Equation (7) for a selected drilled hole, is shown in Figure 10. In Figure 11, the contributions of each energy source (hammer, torque and pull-down) to the SRE total are shown. The type of behaviour shown was consistent throughout the drilling measurements. Regarding the SRE index, it can be noticed that even though the impact (hammer) is dominant, sur-prisingly,

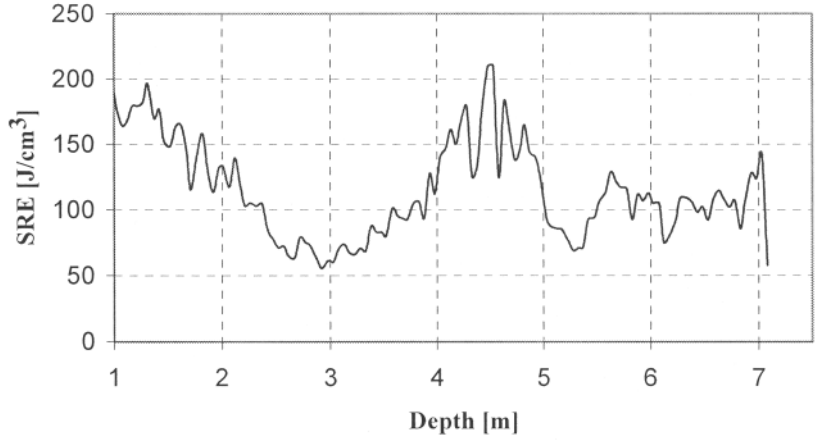

10 SRE profile

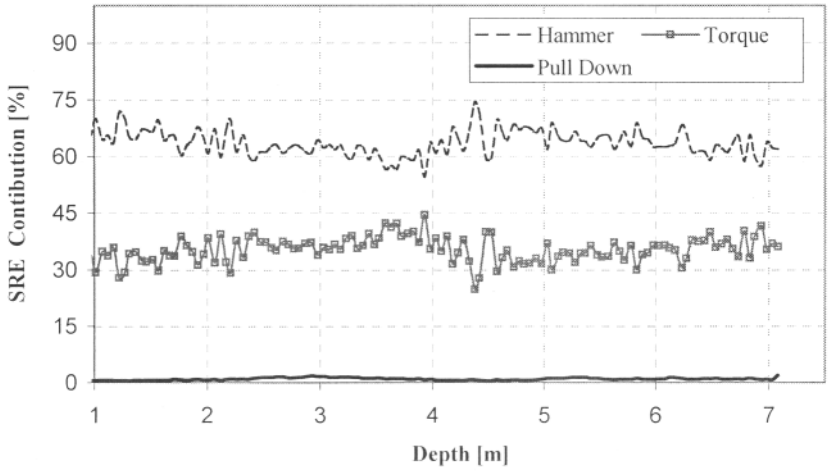

11 Individual source contributions to the SRE

in this case the contribution of the rotation torque amounts to an important fraction of the total SRE, contributing as much is 30%. It is important to note that some rocks will not allow such high torque input because of the danger of stalling. Also, if the hole is deep, torsional elasticity may become an issue limiting the amount of torque that can be applied. In this particular case, the magnitude of the torque contribution may look at first inordinately high; however, the values measured are of the same order of magnitude as those obtained by Ming[13] in a study of vibration in DTH rock drilling. Also, it can be seen that the pull-down contribution to the energy transferred to the rock is small in comparison to the impact and rotation sources.

Correlation between torque and penetration rate

A correlation between the external rotation torque and the average penetration rate has also been noticed in our measurements. As shown in Figure 12, obtained by discretisations in torque increments of 100 Nm, it was found that as the average penetration rate increases, the rotation torque increases. Schunnesson[19,20] observed the same behaviour, and we agree with his explanation that when the rock becomes less competent the bit buttons (inserts), on the average, have a tendency to penetrate deeper into the rock. For this reason, the torque required to rotate the bit increases.

Correlation involving impact frequency

Another interesting correlation found in this study relates the frequency of the hammer and the penetration rate. As shown in Figure 13, an increment in the penetration rate produces a decrease in the impact frequency. This can be explained because when the rock is less competent, the elastic recovery will be lower because more of the energy that initially arrives at the rock is actually absorbed by the rock. If there is less reflected energy, the piston will have a lower reflected velocity. Therefore, the piston will take longer to complete its return stroke because it begins the cycle at a lower velocity. The longer duration of the return stroke will consequently cause a decrease in impact frequency.

Additionally and for the same reasons explained above, a correlation between the frequency and the SRE index was found. The behaviour is such that when the SRE index increases the frequency increases and *vice versa*[9] as shown in Figure 14.

CONCLUSIONS

In the present study, the SRE index is developed using DTH drill monitoring data. This is not a simple task because it is necessary to account for the energy supplied by three separate sources – impact, rotation and pull-down – and then determine the energy effectively transmitted to the rock. It is necessary to

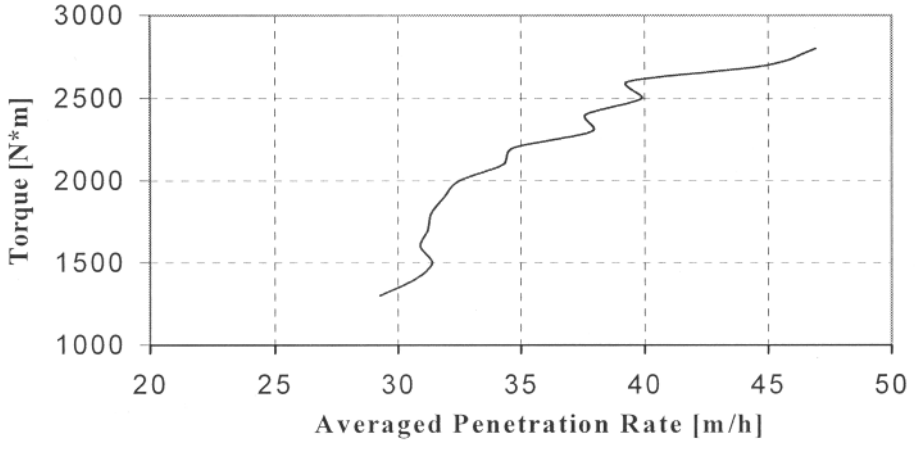

12 Correlation between torque and penetration rate

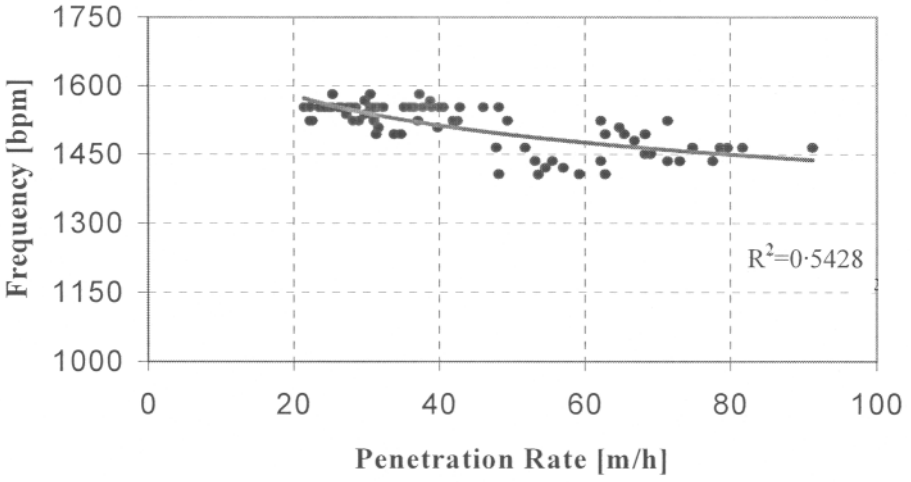

13 Correlation between frequency and penetration rate (bpm, blows per minute)

correct the experimental data to make it rock-dependent only, and in this way meaningful results can be obtained. Thus, an in-depth knowledge of the DTH hammer drilling operation is required.

If the SRE index can be computed from drill monitoring data, then it can be used as a local drillability index to map and characterise the rock at a given drilling site. Measured variations in the value of the index can be helpful in identifying the boundaries between different rock formations. It also can be indicative of a rock mass with a high degree of geological alteration, something that often occurs in mineral deposits.

It was found that a correlation exists between the SRE index and the penetration rate, as well as between the SRE index and the impact frequency.

Additionally, this study has shown two interesting correlations between DTH hammer operational variables. The first is between frequency and penetration rate, where for an increasing penetration rate the frequency drops. This is thought to occur because large penetration rates are normally associated with less competent rock and low elastic recovery. In this case, the reflected speed of the piston after impact is lower so that the return stroke takes longer; therefore, the frequency of operation is reduced. Thus, the variation of hammer frequency could give important information on the rock mass being drilled, at least in terms of the energy absorption characteristics. A second correlation was observed between penetration rate and torque. The torque increases when the penetration rate increases. This is thought to happen because in softer rock, the average indentation depth of the bit buttons into the rock is larger and, therefore, it requires more torque to rotate at the same speed.

It was also found that correlations do exist between the SRE index and the penetration rate, as well as between the SRE index and the impact frequency.

Finally, this work is a contribution towards improving the performance of rock drilling impact hammers and reducing operational costs because the information generated can be used in conjunction with simulation models such as that developed by the authors in order to optimise hammer settings from a design or operational perspective.

ACKNOWLEDGEMENTS

The authors would like to thank Drillco Tools for funding this research and Dr William Hustrulid for his valuable comments and suggestions.

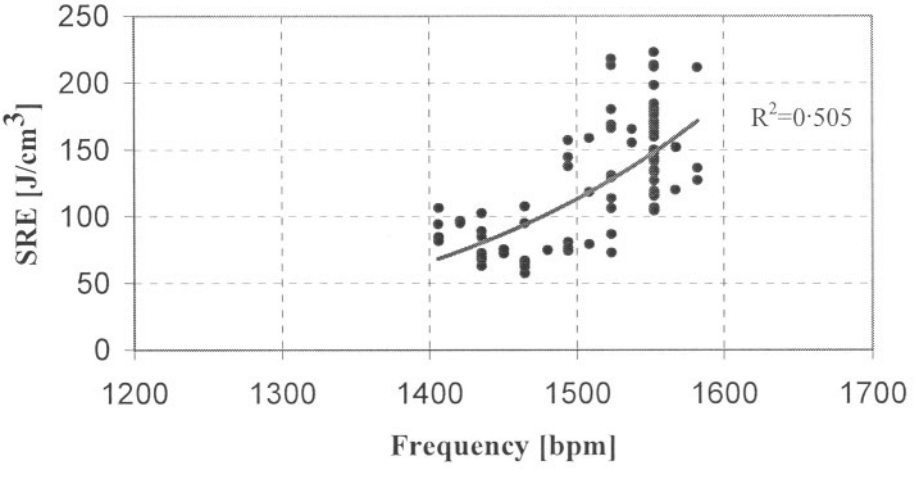

14 Correlation between frequency and the SRE index

REFERENCES

1. L. ATLAS, G. BERNARD and S. NARAYANA: 'Applications of time–frequency analysis to signals from manufacturing and machine monitoring sensors', *Proc. IEEE*, 1996, **84**, 1319–1329.
2. W. CHANGMING and T. SINKALA: 'Thrust: a key parameter in automatic control of percussive drilling', Proceedings of the International Symposium on Mine Mechanization and Automation, Colorado School of Mines, Vol. 1. Golden, Colorado, USA, 1991, 8(11-20).
3. L. CHIANG and D. ELÍAS: 'A study on the thrust effect in the stress wave propagation in down-the-hole rock drilling, 4th World Congress on Computational Mechanics, IACM, Vol. 2, Buenos Aires, Argentina, June, 1998, 1063–1068.
4. L. CHIANG and D. ELÍAS: 'Modeling impact in down-the-hole rock drilling. *Int. J. Rock Mech. Min. Sci.*, 2000, **37**, 599–613.
5. L. CHIANG and E. STAMM: 'Design optimization of valveless DTH pneumatic hammers by a weighted pseudo-gradient search method, ASME', *J. Mech. Design*, 1998, **120**, 687–694.
6. N. DJORDJEVIC: 'Time–frequency analysis of blast induced vibration', *Min. Technol. (Trans. Inst. Min. Metall. A)*, 1999, **108**, A139–A142.
7. W. HUSTRULID: 'Theoretical and experimental study of percussive drilling of rock', Unpublished PhD Thesis, University of Minnesota, 1968.
8. W. HUSTRULID: 'A theoretical and experimental study of percussive drilling of rock', *Int. J. Rock Mech. Min. Sci.*, 1971, **8**, 311–333.
9. L. IZQIERDO: 'Monitoring, analysis ,and characterization of roto-percusive rock drilling systems (in Spanish)', Unpublished MSc thesis, Department of Mechanical Engineering, Pontificia Universidad Catolica de Chile, Chile, 2001.
10. B. LUNDBERG: 'Microcomputer simulation of stress waves energy transfer to rock in percussive drilling', *Int. J. Rock Mech. Min. Sci.*, 1982, **19**, 229–239.
11. B. LUNDBERG: 'Computer modelling and simulation of percussive drilling of rock', (ed. J. Hudson), Comprehensive rock engineering, Vol. 4, 1993, 137–154.
12. B. LUNDBERG and L. KARLSSON: 'Influence of geometrical design on the efficiency of a simple down-the-hole percussive drill', *Int. J. Rock Mech. Min. Sci.*, 1986, **23**, 281–287.
13. J. MING: 'Theoretical and experimental studies of ITH percussive drill vibration', Unpublished MSc thesis, Department of Mining and Metallurgical Engineering, McGill University, Canada, 1994.
14. S. PANG: 'Investigations of pneumatic percussive processes involving rocks', Unpublished PhD thesis, Mechanical Engineering Department, University of California at Berkeley, 1987.
15. J. PECK: 'Performance monitoring of rotary blast hole drills', Unpublished PhD thesis, McGill University, Montreal, Canada, 1989.
16. G. PROAKIS and D. MANOLAKIS: 'Digital signal processing: principles, algorithms and applications', 3rd edn, New York, Prentice-Hall, 1995.
17. H. P. ROSSMANITH, L. MISHNAEVSKY JR, R. E. KNASMILLNER and K. UENISHI: 'Numerical simulation of dynamic fracture and damage of rock during impact', (eds. M. Cerrolaza, C. Gajardo, C. A. Brebbia), Numerical methods in engineering simulation, 1996, 148–154.
18. H. SCHUNNESSON: 'RQD predictions based on drill performance parameters', *Tunnel. Underground Space Technol.*, 1996, **11**, 345–351.
19. H. SCHUNNESSON: 'Drill process monitoring in percussive drilling for location of structural features, lithological boundaries and rock properties, and for drilling productivity evaluation', Unpublished PhD thesis, Luleå University of Technology, Sweden, 1997.
20. H. SCHUNNESSON: 'Rock characterisation using percussive drilling', *Int. J. Rock Mech. Min. Sci.*, 1998, **35**, 711–725.
21. R. TEALE: 'The concept of specific energy in rock drilling', *Int. J. Rock Mech. Min. Sci.*, 1965, **2**, 711–725.
22. K. THURO: 'Prediction of drillability in hard rock tunnelling by drilling and blasting', Proceedings of the World Tunnel Congress '97, Vol. 1, Vienna, Austria, 1997, 103–108.
23. K. THURO and G. SPAUN: 'Introducing the destruction work as a new rock property of toughness refering to drillability in conventional drill and blast tunnelling', (ed. G. Barla), Prediction and performance in rock mechanics and rock engineering. Eurock '96, Vol. 2, Turin, Italy, 1996, 707–713.

Authors

Luis E. Izquierdo was awarded a Master of Engineering Science degree from the Catholic University of Chile in 2001. He is currently employed as lecturer/researcher in the Mechanical Engineering Department of the Catholic University of Chile.

Luciano E. Chiang was awarded a MSc in Mechanical Engineering, a MSc in Electrical Engineering, and a PhD in Mechanical Engineering from Stanford University, USA, in 1983, 1988 and 1989, respectively. He is an Associate Professor and currently the Chairman of the Mechanical Engineering Department of the Catholic University of Chile.

APPENDIX A: Thermodynamic DTH model

See next page

APPENDIX A: Thermodynamic DTH model

Dynamic model

The hammer components are basically two chambers – the piston and the bit. As the air enters the chambers (Fig. A1), the piston will be moved due to the pressure of each chamber.

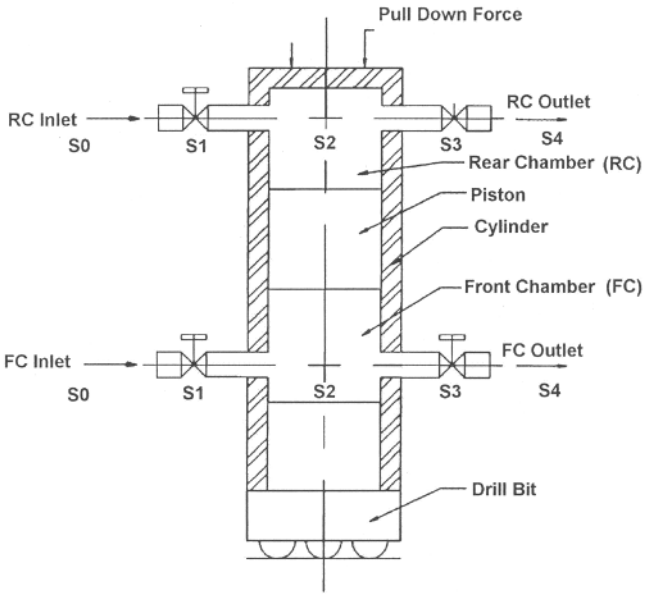

A1 DTH hammer schematics

Nomenclature

x_p, $\dot{x}_p$, piston position and velocity with respect to the impact plane

v_p, $\dot{v}_p$, piston velocity and acceleration with respect to the impact plane

A_{d1RC}, A_{d3RC}, rear chamber input discharge area (d1RC), output discharge area (d3RC)

A_{d1FC}, A_{d3FC}, front chamber input discharge area (d1FC), output discharge area (d3FC)

A_{FP}, A_{RP}, piston front and rear area

C_{RC}, C_{FC}, polytropic expansion constant

e, restitution coefficient

$\dot{m}_{iFC}$, $\dot{m}_{iRC}$, air mass flow at point i of the front chamber (FC) and rear chamber (RC)

m_b, bit mass

m_p, piston mass

n, polytropic expansion coefficient

p^*_{iFC}, p^*_{iRC}, critical air pressure at point i of the front chamber (FC) and rear chamber (RC)

p_{iFC}, p_{iRC}, air pressure at point i of the front chamber (FC) and rear chamber (RC)

p_{d1}, p_{d3}, discharge pressure at points 1 and 3

R, air constant for ideal gas law

T_{iFC}, T_{iRC}, air temperature at point i of the front chamber (FC) and rear chamber (RC)

v_{iFC}, v_{iRC}, air specific volume at point i of the front chamber (FC) and rear chamber (RC)

v_b, bit velocity

v_{pA}, v_{pB}, piston impact and reflected velocity

V_{mfront}, passive volume of the front chamber

V_{mrear}, passive volume of the rear chamber.

Set of differential equations

$$\dot{x}_p = v_p$$

$$\dot{v}_p = \frac{1}{m_p}\left(p_{2FC}\,A_{FP} - p_{IC}\,A_{IC} - p_{2RC}\,A_{rRP} - m_{ps}\right)$$

$$\dot{m}_{2FC} = \dot{m}_{1FC} - \dot{m}_{3RC}$$

$$\dot{T}_{2FC} = \frac{1}{m_{2FC}}\left(-\dot{m}_{2FC}\,T_{2FC} + \dot{m}_{1FC}\,T_{1FC} - \dot{m}_{3FC}\,T_{3FC}\right) - \frac{p_{2FC}\,A_{FP}\,v_p}{m_{2FC}\,c_p}$$

$$\dot{m}_{2FC} = \dot{m}_{1RC} - \dot{m}_{3RC} \qquad \text{Eq. (A1)}$$

$$\dot{T}_{2RC} = \frac{1}{m_{2RC}}\left(-\dot{m}_{2RC}\,T_{2RC} + \dot{m}_{1RC}\,T_{1RC} - \dot{m}_{3RC}\,T_{3RC}\right) - \frac{p_{2RC}\,A_{RP}\,v_p}{m_{2RC}\,c_p}$$

Front chamber non-linear algebraic equations

$$V_{2FC} = V_{mfront} + A_{FP}\,x_p \qquad \text{Eq. (A2)}$$

$$v_{2FC} = \frac{V_{2FC}}{m_{2FC}} \qquad \text{Eq. (A3)}$$

If the outlet sections of the front chamber are closed, then:

$$p_{2FC} = \frac{C_{FC}}{v^n_{2FC}} \qquad \text{Eq. (A4)}$$

$$T_{2FC} = \frac{P_{2FC}\,v_{2FC}}{R} \qquad \text{Eq. (A5)}$$

else

$$p_{2FC} = \frac{RT_{2FC}}{v_{2FC}} \qquad \text{Eq. (A6)}$$

$$C_{FC} = p_{2FC} v^n_{2FC} \qquad \text{Eq. (A7)}$$

The critical pressure at the inlet section is given by:

$$p^*_{1FC} = p_{0FC}\left(\frac{2}{n+1}\right)^{\frac{n}{n-1}} \qquad \text{Eq. (A8)}$$

The actual pressure at the inlet throat P_{d1} is now computed. If [equation] then [equation], otherwise $p_{d1} = p_{2FC}$. Thus:

$$\dot{m}_{1FC} = c_{m1FC}\,A_{d1FC}\left[\frac{2c_p\,p_{0FC}}{Rv_{0FC}}\left(\left(\frac{p_{d1}}{p_{0FC}}\right)^{2/n} - \left(\frac{p_{d1}}{p_{0FC}}\right)^{(n-1)/n}\right)\right]^{1/2} \qquad \text{Eq. (A9)}$$

The critical pressure at the outlet section is given by:

$$p^*_{3FC} = p_{2FC}\left(\frac{2}{n+1}\right)^{\frac{n}{(n-1)}} \qquad \text{Eq. (A10)}$$

The actual pressure at the inlet throat P_{d3} is now computed. If [equation] then [equation], otherwise $p_{d3} = p_{4FC}$. Thus:

$$\dot{m}_{3FC} = c_{m3FC}\, A_{d3FC} \left[\frac{2c_p\, p_{FC}}{R v_{2FC}} \left(\left(\frac{p_{d3}}{p_{2FC}} \right)^{2/n} - \left(\frac{p_{d3}}{p_{2FC}} \right)^{(n-1)/n} \right) \right]^{1/2} \qquad \text{Eq. (A11)}$$

Rear chamber non-linear algebraic equations
Rear chamber equations are the same as frontal ones.

Analysis of the piston
Linear conservation of momentum

$$m_p\, v_{pA} = m_p\, v_{pB} + m_b\, v_{bB} \qquad \text{Eq. (A12)}$$

Energy conservation

$$\frac{1}{2} m_p\, v_{pA}^2 = \frac{1}{2} m_p\, v_{pB}^2 + \frac{1}{2} m_b\, v_{bB}^2 \qquad \text{Eq. (A13)}$$

thus

$$v_{pB} = \frac{m_b - m_p}{m_b + m_p}\, v_{pA} \qquad \text{Eq. (A14)}$$

and

$$v_{bB} = \frac{2m_p}{m_b + m_p}\, v_{pA} \qquad \text{Eq. (A15)}$$

The energy absorbed by the rock is the kinetic energy transmitted by the bit by the impact

$$E_R = \frac{1}{2} m_b\, v_{bB}^2 \qquad \text{Eq. (A16)}$$

The energy reflected through the piston is:

$$E_p = \frac{1}{2} m_p\, v_{pB}^2 \qquad \text{Eq. (A17)}$$

Thus, the energy lost by the piston could be estimated by:

$$E_{Lp} = \frac{1}{2} m_p \left(v_{pA}^2 - e^2 \right) \qquad \text{Eq. (A18)}$$

APPENDIX B: Impact simulation

Stress wave computation using nodes
The computation of the stress wave propagation is divided into time intervals. At the beginning of every time interval, the principle of linear momentum conservation is applied to each node (Fig. B1). We can obtain an expression for the new node velocity V_N that is computed as a function of the connecting elements, force and velocity, at the previous time interval.

$$V_N = \frac{\rho a \left(A_L V_L + A_R V_R \right) + P_L - P_R + P_T}{\rho a \left(A_L + A_R \right)} \qquad \text{Eq. (B1)}$$

Applying the same linear momentum principle both to the left part and to the right sides of the node, the magnitude of forces reflected at the node can be evaluated according to Equation (B2), P_{NL} (force propagated towards the left) and P_{NR} (force propagated towards the right).

$$P_{NL} = \rho a A_L \left(V_L - V_N \right) + P_L$$

and

$$P_{NR} = \rho a A_R \left(V_N - V_R \right) + P_R \qquad \text{Eq. (B2)}$$

Note that if more than two elements connect to one node, Equation (B1) should be modified accordingly. For example, at the interface between the drill bar and the drill bit shown in Figure B2, if the gap in between is null then the equation for the node velocity is:

$$V_N = \frac{\rho a \left(A_b V_b + A_L V_L + A_R V_R \right) + P_L + P_b - P_R + P_T}{\rho a \left(A_L + A_R \right)} \qquad \text{Eq. (B3)}$$

In addition, in this case the forces reflected at the node can be computed as:

$$P_{Nb} = \rho a A_b \left(V_b - V_N \right) + P_b$$

and

$$P_{NR} = \rho a A_R \left(V_N - V_R \right) + P_R \qquad \text{Eq. (B4)}$$

Stress-wave computation at elements
On each element, the velocity is calculated at the end of the time interval using the following equation:

$$V_E = \frac{\rho a A_E \left(V_{NL} - V_{NR} \right) + P_{NL} - P_{NR}}{2 \rho a A_E} \qquad \text{Eq. (B5)}$$

$$P_E = P_{NL} + \rho A_E\, a \left(V_{NL} - V_E \right) \quad \text{or}$$
$$P_E = P_{NR} + \rho A_E\, a \left(V_E - V_{NR} \right) \qquad \text{Eq. (B6)}$$

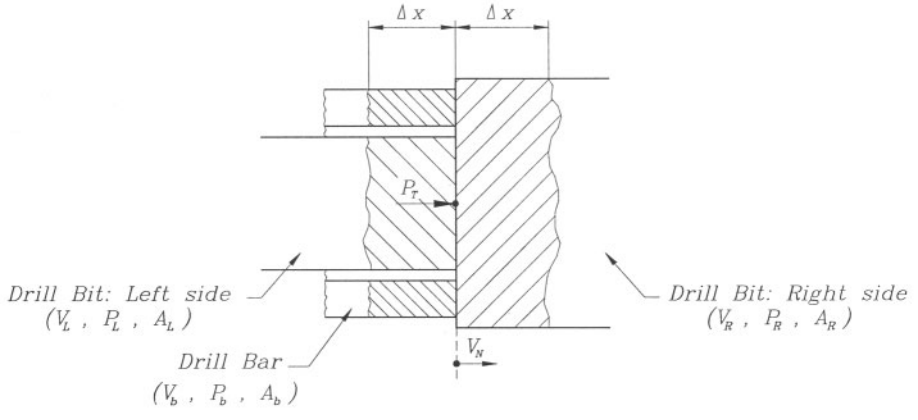

B1 Drill bar–drill bit interface

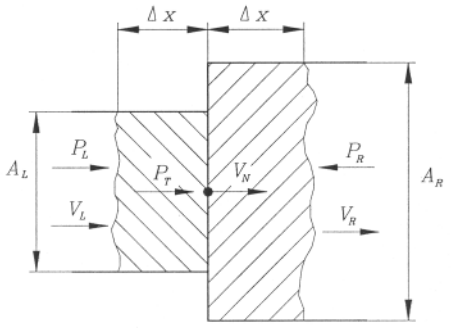

B2 Linear momentum principle applied to a node between times t^- and t^+

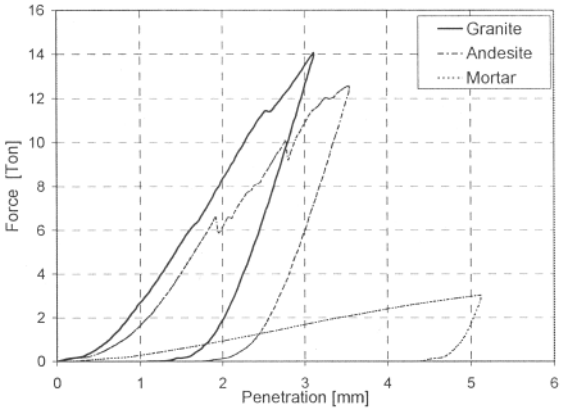

B3 Experimental force penetration curve

Solid body interfaces

A gap element was use to model the interface between elastic solid bodies. When two elastic solid bodies are in contact, the gap element transmits the forces from the end node of one body to the end node of the second body and *vice versa*.

Rock interaction

The rock behaviour during impact is a very complex subject because of its non-linearity, and because the contact geometry between tungsten carbide inserts and the rock is also complex. Essentially, in our method, the rock behaviour is introduced as a boundary condition in the form of a force–penetration law. This is derived experimentally for every different combination of drill bit and rock that is of interest (Fig. B3).